Beyond boron–oxygen deactivation: Industrially feasible LID-free p-type Czochralski silicon

Bianca Lim[1], Agnes Merkle[1], Robby Peibst[1,2], Thorsten Dullweber[1], Yichun Wang[3] & Rui Zhou[3]
[1]Institute for Solar Energy Research Hamelin (ISFH), Emmerthal, Germany
[2]Institute of Electronic Materials and Devices, Leibniz Universität Hannover, Hanover, Germany
[3]LONGi Clean Energy Technology Co., Ltd., Xi'an City, China

Abstract

Today's industry-standard B-doped monocrystalline silicon still suffers from light-induced degradation (LID) of the carrier lifetime. Illumination at elevated temperatures leads to a so-called *regeneration*, i.e. a recovery of both the carrier lifetime and the solar cell efficiency. However, even though the carrier lifetime on test wafers increases from about 1ms after processing to 3ms after regeneration, the corresponding PERC+ cell efficiencies in both states are identical; possible reasons for this discrepancy are discussed in this paper. Additionally, B-doped Czochralski silicon wafers with an ultralow oxygen content of 2.6 ppma are evaluated, as well as industrial Ga-doped wafers. Both wafer materials are completely LID free, as demonstrated in lifetime measurements and PERC+ cell efficiencies, and enable up to 0.4%$_{abs.}$ higher efficiencies than current industry-typical boron-doped wafers.

Introduction

About 35% of current global PV production uses B-doped monocrystalline silicon (c-Si) [1]. Advances in the Czochralski (Cz) process, i.e. the crystal growth technique, have resulted in ever-better material quality and ever-lower prices. This in turn supports the roll-out of high-efficiency passivated emitter and rear cells (PERCs), which already yield efficiencies of up to 21.5–22.0% in mass production when using Cz-Si [2–5].

Yet, despite all advances, industrial B-doped Cz-Si still contains significant amounts of interstitial oxygen. This, in combination with the boron doping, results in light-induced degradation (LID) of the carrier lifetime and, in turn, the solar cell efficiency.

Boron–oxygen (BO)-related LID was first reported in 1973 [6] and was studied in detail in the late 1990s and early 2000s. As this degradation is firmly linked to the simultaneous presence of both boron and oxygen [7,8], two straightforward ways to avoid it are to either reduce the interstitial oxygen content or replace boron as a dopant (e.g. with Ga for p-type or with P for n-type wafers) [7,9].

One way to produce low-oxygen Cz-Si is to employ a strong magnetic field during the silicon crystal growth process [10]; however, this technology has not entered mass production, probably because production costs are too high. Replacing boron with gallium is not as straightforward as it sounds either; using standard Czochralski processes for Ga-doped ingots results in a very large increase in doping concentration along the ingot.

"Despite all advances, industrial B-doped Cz-Si still contains significant amounts of interstitial oxygen."

A third option to mitigate LID due to BO-related defects is the permanent deactivation of these defects, which can be done by generating excess carriers at elevated temperatures, e.g. by illumination. The resulting regeneration of the solar cell characteristics and the carrier lifetime was first reported in 2006 [11]. The process can be employed with all B-doped Cz-Si materials and solar cells; however, the effectiveness of regeneration depends on a variety of material and process parameters.

In work reported in this paper, the carrier lifetime, as well as the solar cell efficiency potential of current industry-standard B-doped Cz-Si, is evaluated. For this, dedicated test samples are used for lifetime measurements, along with an in-house PERC+ solar cell baseline process which typically yields energy conversion efficiencies of around 21.5% [12].

Lifetime and efficiency are measured after full LID due to BO-related defects, and after applying an optimized, lab-type regeneration treatment.

The performance of industry-standard B-doped Cz-Si is compared with that of industrial Ga-doped Cz-Si as well as with that of B-doped Cz-Si wafers with ultralow oxygen content. The latter wafers result from an advanced pulling technology that is being developed by LONGi as a potential candidate for future mass production of high-quality and low-cost Cz-Si wafers.

The lifetimes measured on dedicated test samples are used as an input parameter for device simulations, and the results are compared with the measured solar cell characteristics. In particular, lifetime and solar cell efficiency are measured in three different states: 1) directly after processing; 2) after 24h of illumination at room temperature (which results in complete LID for the industry-standard B-doped Cz-Si); and 3) after applying the regeneration treatment.

By means of this sequence of measurements, an assessment of the effectiveness of the permanent deactivation of BO-related defects is essentially made, as well as of the extent of LID (if any) in the advanced Cz-Si wafers with Ga doping or ultralow oxygen content. Also investigated is whether there are any other lifetime-limiting defects present in industry-standard B-doped Cz-Si that are not observed in Ga-doped or oxygen-lean B-doped Cz-Si.

Bulk lifetimes of the different Cz-Si wafer materials

Four different Czochralski-grown (Cz) silicon materials from LONGi Clean Energy Technology Co. are studied in terms of stability of the bulk lifetimes. Two of the materials are industrial B-doped Cz-Si with 'standard' interstitial oxygen concentrations of 12 and 16 ppma respectively. The other two materials are assessed as industrial-scale LID-free options; the first is B-doped Cz-Si with an extremely low interstitial oxygen concentration of 2.6 ppma, and the second is Ga-doped Cz-Si from an industrial-type puller. The ultralow oxygen concentration of 2.6 ppma was achieved by using an advanced Cz pulling technology developed by LONGi, which reduces the oxygen dissolution into the silicon melt during crystallization.

Table 1 summarizes the resistivities and interstitial oxygen concentrations (measured by Fourier-transform infrared spectroscopy – FTIR – using the ASTM F121-83 standard) of the four materials. The wafers are of dimension 156.75mm × 156.75mm (M2) and have an initial thickness of around 180µm.

To measure the bulk lifetime, symmetrical test structures are processed. First, the saw damage is removed and the wafers cleaned. The wafers then go through the same $POCl_3$ diffusion that is used for the baseline PERC+ solar cell process. On the one hand, this acts as a gettering step; on the other, it adds to the thermal history of the wafers and keeps it close to that of the PERC+ solar cells. Subsequently, the resulting n^+ regions on both surfaces are etched off and the wafers cleaned, and an AlO_x/SiN_y stack is deposited on the front and the rear for optimal surface passivation.

Finally, the lifetime samples are fired in a belt-firing furnace. Note that there are two groups, which are fired at two different belt speeds: 5.6m/min, which is the speed at which the solar cells are fired, and 6.8m/min, in order to obtain optimum lifetimes after regeneration [13].

After firing, the lifetime samples are in the 'as-processed' state. The carrier lifetimes are then measured with a WCT-120 Lifetime Tester from Sinton Instruments, both in quasi-steady state and in photoconductance decay mode.

Next, the samples are illuminated for 24h at around 0.1 Suns and at room temperature to activate the BO-related defects. With regard to the bulk resistivity values of up to 2.1Ωcm, 24h was chosen in order to reach saturation of LID [14]; at this point, the lifetime is measured again.

Finally, the regeneration treatment is applied, and the lifetime measured for a third time. The lab-type regeneration process consists of annealing on a hotplate set to 185°C and simultaneously illuminating with a halogen lamp at a light intensity of around 1 Sun for 15 min. It is important to note that it was verified that no further increase in lifetime is observed when annealing under illumination for longer times.

The lifetimes of the four different materials in the three different states are plotted in Figs. 1 and 2. Figs. 1(a) and 2(a) depict the effective lifetimes of inherently LID-free Cz-Si materials, while Figs. 1(b) and 2(b) show the significant changes that happen in B-doped Cz-Si with an industrially typical interstitial oxygen concentration.

Note that Fig. 1 contains the materials with slightly higher resistivities (1.7 and 2.1Ωcm), while Fig. 2 depicts the materials with lower resistivities (1.1 and 1.0Ωcm). The materials are grouped like this because material quality, or rather solar cell potential with regard to material quality, is determined by lifetime as well as resistivity. One can therefore only easily compare lifetimes of materials with similar doping concentrations.

The blue triangles in the graphs correspond to the measured lifetimes after the fast-firing step (as-processed). The red circles give the lifetimes after illumination at room temperature for 24h, i.e. in the case of the B-doped samples after LID. The green diamonds refer to the lifetimes after applying the regeneration treatment (annealing under illumination at 185°C for 15 min). In addition, all graphs contain the respective intrinsic lifetime according to the model of Richter et al. [15] (solid black line).

Fig. 1(a) depicts the effective lifetimes of the 2.1Ωcm B-doped material with ultralow interstitial oxygen concentration of 2.6 ppma. As expected, no LID of the bulk carrier lifetime is observed between the as-processed and the degraded state [16]. However, applying the regeneration treatment improves the lifetime from around 2ms to around 3.8ms at an excess carrier concentration $\Delta n = 10^{15}cm^{-3}$.

For the B-doped 1.7Ωcm sample, the lifetimes measured after firing at different belt speeds are plotted in Fig. 1(b). The open symbols correspond to the effective lifetimes measured after firing at a belt speed of 5.6m/min, and the filled symbols correspond to a belt speed of 6.8m/min. For the slower belt speed, the as-processed lifetime (open blue triangles) at an excess carrier concentration of $\Delta n = 10^{15}cm^{-3}$ is around 650µs. After 24h of illumination at room temperature, the lifetime drops to around 200µs (degraded state, open red circles), and after application of the regeneration treatment, the lifetime increases to around 1.4ms (regenerated state, open green diamonds).

Using a faster belt speed during the fast-firing process notably increases the effective lifetimes in all three states. An as-processed (filled blue triangles) lifetime of 1.1ms at $\Delta n = 10^{15}cm^{-3}$ is measured. In the degraded state (filled red circles), the lifetime is

No.	Dopant species	Resistivity [Ωcm]	$[O_i]$ [ppma]
1	B	1.7	~16
2	B	1.1	~12
3	B	2.1	2.6
4	Ga	1.0	~16

Table 1. Dopant species, resistivity ρ and interstitial oxygen concentration $[O_i]$ for each of the four different Cz-Si materials investigated.

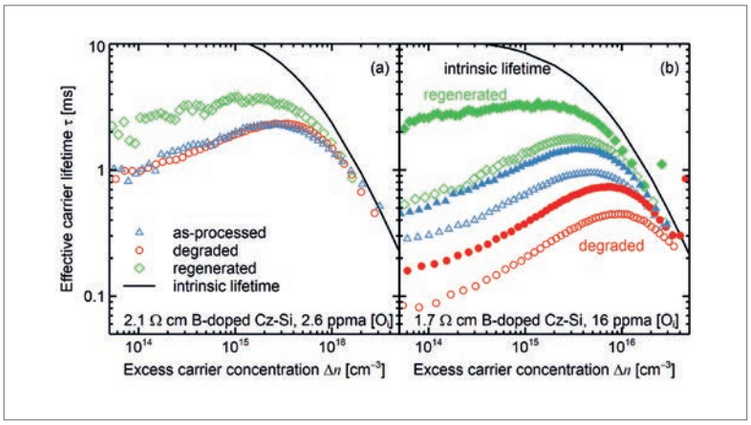

Figure 1. Effective lifetimes as a function of excess carrier concentration: (a) 2.1Ωcm, ultralow $[O_i]$ B-doped Cz-Si; (b) 1.7Ωcm industry-standard B-doped Cz-Si. The blue triangles represent the as-processed state, the red circles the degraded state, and the green diamonds the regenerated state. The open symbols denote a belt speed during fast-firing of 5.6m/min, while the filled symbols indicate a belt speed of 6.8m/min. The solid black line marks the intrinsic lifetime limit according to Richter et al. [15] for the given resistivity.

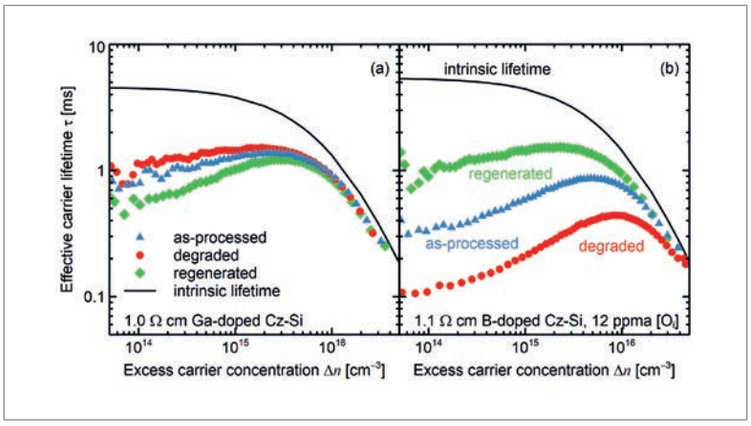

Figure 2. Effective lifetimes as a function of excess carrier concentration: (a) 1.0Ωcm Ga-doped Cz-Si; (b) 1.1Ωcm industry-standard B-doped Cz-Si. The wafers are fired at a belt speed of 6.8m/min. The blue triangles signify the as-processed state, the red circles the degraded state, and the green diamonds the regenerated state. The solid black line marks the intrinsic lifetime limit according to Richter et al. [15] for the given resistivity.

"Industry-standard B-doped Cz-Si wafers perform as well as the inherently LID-free materials with similar doping concentrations."

around 390µs, and regeneration results in an effective lifetime of 3.2ms at $\Delta n = 10^{15}cm^{-3}$ (filled green diamonds), which is comparable to the lifetime measured on the ultralow $[O_i]$ Cz-Si.

While such a dependence of the lifetime on the belt speed during fast firing was already shown in Walter et al. [17], it should be noted that this was not observed at ISFH for all B-doped Cz-Si materials. The ultralow $[O_i]$ Cz-Si, for example, yields similar lifetimes after firing at 5.6m/min and 6.8m/min (not shown here).

The fact that even the regenerated lifetime curves are below the intrinsic lifetime published by Richter et al. [15] (solid black line) can be attributed to surface recombination. Assuming a surface recombination velocity of just 2cm/s per side already closes the gap between measured lifetime and intrinsic model; this is a reasonable value for the AlO_x/SiN_y stack used.

On inspection of the measured lifetimes of the Ga-doped Cz-Si (Fig. 2(a)), only small changes are seen, as might be expected. A period of 24h of illumination at room temperature (red circles) actually results in slightly higher lifetimes than those measured in the as-processed state (blue triangles). After the regeneration treatment, however, a slight decrease in the lifetime is seen, especially at excess carrier densities below $5\times10^{15}cm^{-3}$ (green diamonds). This might be a bulk effect, but could also be related to a degradation in the surface passivation quality. However, it needs to be proved with larger wafer numbers whether or not the slight lifetime degradation after regeneration is statistically significant.

In contrast, for the industrial 1.1Ωcm Cz-Si with an interstitial oxygen concentration of 12 ppma (Fig. 2(b)), the lifetime changes significantly. Approximately 600µs was measured in the as-processed state at $\Delta n = 10^{15}cm^{-3}$, 210µs after LID, and around 1.4ms after regeneration.

When the injection-dependent bulk lifetimes measured after applying the regeneration treatment are compared, it is seen that the industry-standard B-doped Cz-Si wafers perform as well as the inherently LID-free materials with similar doping concentrations. One would therefore also expect a similar solar cell performance after permanent deactivation of the BO defect.

Higher PERC+ conversion efficiencies on completely LID-free Cz-Si wafer materials

The four above-mentioned Cz-Si materials were used to process bifacial PERC+ solar cells. The PERC+ process sequence is described in detail in Dullweber et al. [18]; however, here, just the basic process flow will be highlighted.

The PERC+ process starts with saw-damage removal and wafer cleaning. A rear protection layer is then applied to act as an etching and diffusion barrier during the subsequent front-surface texturing and phosphorus diffusion steps. After this, the PSG and protection layer are removed, and a stack of aluminium oxide (AlO_x) and plasma-enhanced chemical vapour deposited (PECVD) silicon nitride (SiN_y) is applied to passivate the rear side. PECVD-SiN_y is also deposited on the front to passivate the P-doped emitter and act as an anti-reflection coating.

To enable contact formation on the rear side, the AlO_x/SiN_y stack is locally removed using a picosecond laser with a wavelength of 532nm, before Al fingers are screen printed on the rear side and Ag fingers on the front. At the end of the sequence, the metal pastes are co-fired in a belt-firing furnace with a belt speed of 5.6m/min. A schematic of the final solar cell structure is shown in Fig. 3.

The *I–V* curves of the solar cells are measured using a LOANA system from pvtools. As in the case of the dedicated lifetime samples, the solar cells are measured: 1) directly after processing; 2) after illumination at room temperature for 24h; and 3) after applying the regeneration treatment.

The results of the measurements are shown in Fig. 4; the solar cell efficiencies have been plotted for the different materials in the as-processed state relative to the efficiency of the industrial 1.7Ωcm B-doped Cz-Si with 16 ppma $[O_i]$ (green diamonds). The change due to illumination at room temperature and the change after applying the regeneration treatment are plotted relative to the respective as-processed efficiencies.

After processing, the efficiency of the PERC+ solar cells with 2.6 ppma $[O_i]$ (blue squares) is $0.4\%_{abs.}$ higher than that of the cells using the industrial 16 ppma $[O_i]$ Cz-Si. Similarly, the solar cells from the Ga-doped Cz-Si (open red circles) perform $0.3\%_{abs.}$ better than the industry-standard B-doped Cz-Si with similar doping concentrations (purple triangles). On an absolute scale, the PERC+ conversion efficiencies range between 21.0 and 21.5% in a five-busbar design. With a busbar-less design and R&D-type Ga wafers similar to material 4 in Table 1, the best PERC+ efficiency is 22.1% [16].

As expected from the lifetime measurements, the solar cell efficiency of the ultralow $[O_i]$ B-doped as well as the Ga-doped cells is not affected by either illumination at room temperature or illumination at elevated temperature (within the measurement uncertainty), and hence the cells are completely LID free [16].

In contrast, the PERC+ solar cells from industrial B-doped Cz-Si degrade by $0.5–0.7\%_{abs.}$ after 24h of illumination at room temperature, widening the gap to the LID-free materials to $0.8–1.1\%_{abs.}$. After the regeneration treatment is applied, the measured efficiencies improve, but only to a similar level to that before LID, and no higher.

The efficiency gap between the inherently LID-free materials and the industrial B-doped Cz-Si after regeneration seems to be in disagreement with the lifetime measurements: here, the lifetime of the industrial B-doped materials after regeneration was similar to that of the ultralow [O_i] and the Ga-doped Cz-Si.

Device simulations: Translating bulk lifetimes to solar cell efficiencies

In order to understand the discrepancy discussed in the previous section, a device simulation was set up using the conductive boundary model [19], as implemented by the Quokka 2 computer simulation program in Fell [20]. The input parameters, which are based on an extensive characterization of ISFH's baseline PERC+ solar cell process, are summarized in Table 2. The injection-dependent lifetimes of the B-doped Cz-Si wafers, as measured on the lifetime test structures, can be described by a Shockley-Read-Hall (SRH) defect at mid-gap, with a factor of 10 between τ_{no} and τ_{po}. The table lists the defect lifetimes for the as-processed state of the 1.7Ωcm B-doped sample with 16 ppma [O_i] (material 1). Note that the lifetime measured on the designated test sample that was fired at the same belt speed as the solar cells, i.e. 5.6m/min, was used.

The front-contact shadowing is calculated from the optical finger width and the layout of the front grid. The saturation current density of the emitter J_{oe} is determined on symmetrical test wafers using the Kane and Swanson method. Transmission line model (TLM) measurements were taken to determine the specific contact resistances at the front and rear. The saturation current densities J_o at the contacts are based on lifetime measurements performed on test samples with various metallization fractions, both for the emitter and for the base contact. The depth-dependent generation profile is calculated by parameterizing the measured reflectance of a PERC+ solar cell according to Brendel et al. [21].

The simulation set-up was verified by inserting the effective lifetime measured in the as-processed state for material 1 (1.7Ωcm B-doped with 16 ppma [O_i]) and comparing the result with measured I–V parameters in the as-processed state. The results are summarized in Table 3.

The efficiency η, open-circuit voltage V_{oc} and short-circuit current density J_{sc} are in good agreement with the simulated values, while the measured fill factor FF is 0.45%$_{abs.}$ higher. This is partly the result of a higher pseudo fill factor pFF (0.3%$_{abs.}$) as well as a lower series resistance (~0.05Ωcm^2), but it is nevertheless a fairly good match.

Once the simulation set-up has been verified, the lifetimes measured after process, after illumination at room temperature and after applying the regeneration treatment are inserted. Thus, the efficiency changes that one would expect from the observed lifetime changes can be compared with the actual changes observed on the solar cells. This comparison is performed for materials 1 and 3, i.e. the industry-standard 1.7Ωcm B-doped Cz-Si and the B-doped Cz-Si with extremely low interstitial oxygen concentration.

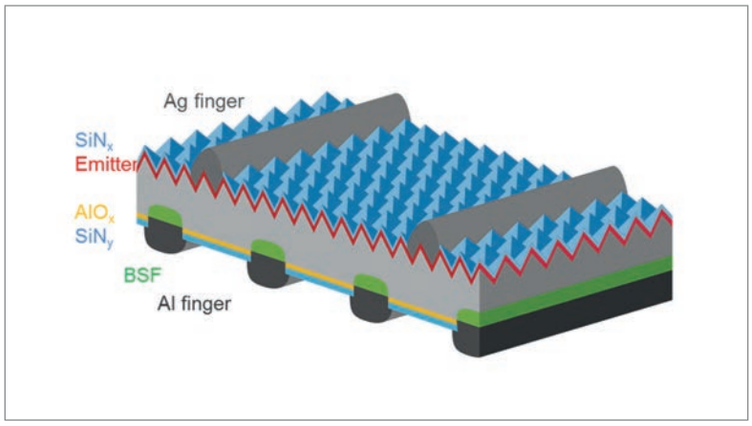

Figure 3. Schematic of a bifacial PERC+ solar cell.

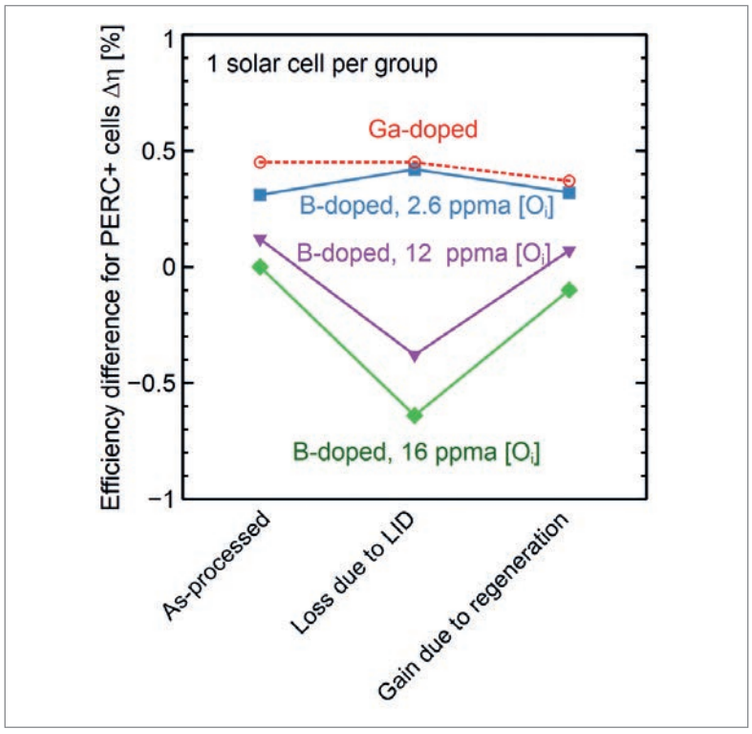

Figure 4. Efficiency differences for the PERC+ solar cells fabricated from the four different Cz-Si materials in the as-processed state, as well as after illumination at room temperature and after applying the regeneration treatment.

The results are shown in Fig. 5. For the as-processed state, the efficiency of the industrial 1.7Ωcm B-doped Cz-Si with 16 ppma [O_i] (green diamonds) is used as the baseline value. The change due to illumination at room temperature and the change after applying the regeneration treatment are plotted relative to the respective as-processed efficiencies. Values corresponding to measured solar cell efficiencies are represented by filled symbols, while the results from the simulation are depicted by open symbols.

As mentioned above, the actual ultralow [O_i] solar cells (orange circles) yield 0.3%$_{abs.}$ higher efficiencies than the solar cells fabricated on industrial B-doped

Parameter	Value
Wafer resistivity	1.7Ωcm
Wafer thickness	170μm
τ_{no} for mid-gap SRH centre	292μs
τ_{po} for mid-gap SRH centre	2,920μs
Front-contact shadowing	4.5%
Emitter sheet resistance R_{sh}	95Ω/sq.
J_{oe} of SiN_y-passivated emitter	100fA/cm^2
J_{oe} below Ag finger contacts	1,000fA/cm^2
Specific contact resistance, front	1.5mΩcm^2
J_o at the passivated rear side	12fA/cm^2
J_o at the Al rear contact	350fA/cm^2
Specific contact resistance, rear	3mΩcm^2

Table 2. Input parameters for the device simulations of PERC+ solar cells using the lifetime data of the B-doped Cz-Si with 16 ppma [O_i] in the as-processed state.

Parameter	Simulation	Measurement
Efficiency η [%]	21.49	21.53
V_{oc} [mV]	669.8	667.3
J_{sc} [mA/cm^2]	39.54	39.53
FF [%]	81.16	81.62
R_s [Ωcm^2]	0.468	0.420
pFF [%]	83.37	83.68

Table 3. Simulated and measured *I–V* parameters for the baseline PERC+ solar cell process and the 1.7Ωcm B-doped Cz-Si with 16 ppma [O_i].

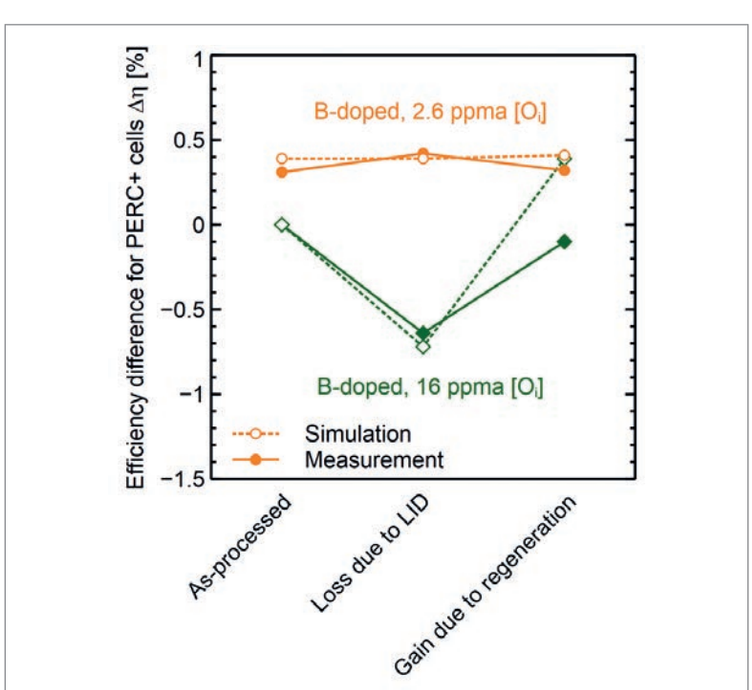

Figure 5. Measured (filled symbols, solid lines) and simulated (open symbols, dashed lines) differences in PERC+ cell efficiency Δη after illumination at room temperature and after applying the regeneration treatment.

Cz-Si (green diamonds) directly after processing. This difference is also predicted by the simulation when the respective effective lifetimes measured in the as-processed state are entered.

Illumination at room temperature notably decreases the lifetime in the 16 ppma [O_i] B-doped Cz-Si. Inserting this degraded lifetime into the simulation yields a 0.7%$_{abs.}$ loss compared with the as-processed state (open green diamonds). This is in good agreement with the degradation observed on actual PERC+ solar cells (filled green diamonds). After regeneration, the measured PERC+ efficiency of the industrial B-doped Cz-Si improves to a similar level to that before LID, whereas the device simulation with the regenerated lifetime predicts an increase by 0.4%$_{abs.}$ compared with before LID.

The measured PERC+ efficiency of the 2.6 ppma [O_i] B-doped material, on the other hand, is stable, during both the degradation and the regeneration treatment (within the measurement uncertainty). This is in accordance with the measured bulk lifetimes, which do not decrease after illumination at room temperature (see Fig. 1(b)). While an increase in bulk lifetime is observed for the 2.6 ppma B-doped Cz-Si after applying the regeneration treatment, this increase only translates to an efficiency gain of 0.02% in the device simulation, as the other recombination channels are much more dominant.

The comparison between measured solar cell efficiencies and efficiencies simulated on the basis of measured bulk lifetimes reveals a notable discrepancy for the regenerated state of the industrial B-doped Cz-Si. The difference in the measured bulk lifetimes in the degraded and the regenerated states should translate to an efficiency gain of 1.1%$_{abs.}$ after regeneration. For the actual solar cells, however, an increase by only 0.7%$_{abs.}$ was observed.

Hence, in contrast to the experimental results, according to the simulation the regenerated industrial B-doped wafer material should enable identical PERC+ efficiencies to those for the ultralow [O_i] wafer material. This suggests that in the case of the industrial B-doped Cz-Si, there is a difference in the regenerated bulk lifetime of the test wafers and the PERC+ solar cells. Since the lifetime test wafers were processed in parallel to the solar cells – as far as possible – this raises the question as to where this difference might stem from.

Possible reasons for lower-than-expected efficiency after regeneration of industry-typical Cz-Si

A look at the detailed processing sequence used in this work reveals three major differences between lifetime test structures and PERC+ solar cells: 1) the solar cells have a rear protection layer during the P-diffusion step; 2) during the fast-firing process, the solar cells have an emitter on the front side; and 3) the solar cells are fired with metal pastes on both surfaces. In contrast, for the lifetime test wafers: 1) the n^+ emitter first forms on both wafer sides;

subsequently, 2) the emitter is removed from both wafer surfaces, which are then passivated with an AlO_x/SiN_y stack; and 3) metal pastes are obviously not applied to the lifetime samples.

With regard to the rear protection layer during P diffusion, experimental results obtained from a different study make it seem unlikely that this has any significant impact. In that study's experiment, the solar cells as well as the lifetime samples were diffused on both surfaces, and the n^+ emitter on the rear was then removed by a rear polishing step. Also in that experiment, the PERC+ cell efficiencies after processing and after regeneration were identical, in contrast to the carrier lifetimes, measured on lifetime samples, which were higher after regeneration.

In respect of the presence of the n^+ emitter during the fast-firing step, the effective lifetimes of non-metallized implied-V_{oc} (iV_{oc}) solar cell precursors were measured and simulated. These are identical to PERC+ solar cells except for the laser contact opening and the screen-printing steps. For the simulation, the front metal recombination was set to be equal to that of the passivated emitter, and the rear metal recombination to be equal to that of the passivated rear side. All other parameters were the same as for the solar cell simulation.

Fig. 6 shows the effective lifetime of such an iV_{oc} precursor. The blue triangles correspond to the as-processed state, and the green diamonds to the regenerated state. The lines indicated the simulated effective lifetimes, i.e. the result of simulating an implied-V_{oc} structure, on the assumption of the bulk lifetime measured in the as-processed (solid blue line) and in the regenerated state (dashed green line).

In the as-processed state, the measured effective lifetime (blue triangles) matches the simulated effective lifetime (solid blue line) very well. The measured effective lifetime on the non-metallized precursor after regeneration (green diamonds), however, is notably lower than the simulated effective lifetime (dashed green line). It therefore seems as if the presence of the n^+ emitter during the fast-firing step negatively affects the bulk lifetime.

A possible reason for the above effect could be related to hydrogen, which interacts with various defects in the silicon bulk. A major source of hydrogen is the SiN_x layer combined with the fast-firing step [22]. The presence of an n^+ emitter, however, affects the transport of hydrogen from the SiN_x into the bulk [23], which could result in different bulk lifetimes in the lifetime test wafers and the solar cell precursors. This aspect is currently undergoing further investigation.

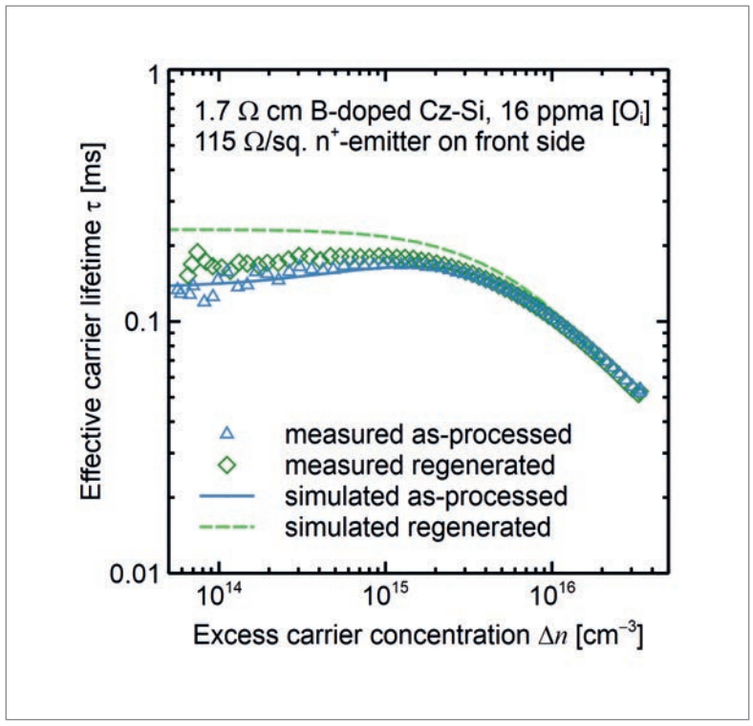

Figure 6. Measured (symbols) and simulated (lines) injection-dependent effective lifetimes of industry-standard 1.7Ωcm B-doped Cz-Si with a SiN_y-passivated 115Ω/sq. n^+ emitter on the front side. The blue triangles and solid blue line correspond to the as-processed state, and the green diamonds and dashed green line to the regenerated state.

References

[1] ITRPV 2018, "International technology roadmap for photovoltaic (ITRPV): 2017 results", 9th edn (Mar.) [http://www.itrpv.net/Reports/Downloads/].

[2] [https://www.pv-magazine.com/2018/01/19/longi-achieves-record-conversion-rate-of-20-41-for-perc-modules/].

[3] JinkoSolar Holding Co., Ltd. 2017, Annual Report.

[4] [https://www.pv-tech.org/news/aiko-solar-enters-volume-production-of-mono-perc-cell-with-22-conversion-ef].

[5] Lee, B.G. et al. 2018, "Development of p-Cz PERC solar cells approaching 23% efficiency for gigawatt-level production", *Proc. 35th EU PVSEC*, Brussels, Belgium, pp. 308–400

[6] Fischer, H. & Pschunder, W. 1973, "Investigation of photon and thermal induced changes in silicon solar cells", *Proc. 10th IEEE PVSC,* Palo Alto, California, USA, p. 404.

[7] Schmidt, J., Aberle, A. & Hezel, R. 1997, "Investigation of carrier lifetime instabilities in Cz-grown silicon", *Proc. 26th IEEE PVSC*, Anaheim, California, USA, pp. 13–18.

[8] Glunz, S.W. et al. 1998, "On the degradation of Cz-silicon solar cells", *Proc. 2nd World Conf. PV Solar Energy Conv.,* Vienna, Austria, p. 1343.

[9] Glunz, S.W. et al. 1999 "Comparison of boron and gallium doped p type Czochralski silicon for photovoltaic application", *Prog. Photovolt: Res. Appl.,* Vol. 7, No. 6, pp. 463–469.

[10] Mosel, F. et al. 2012, "Growth of high quality silicon mono ingots by the application of a magnetic CUSP field in Cz-puller", *Proc. 27th EU PVSEC*, Frankfurt, Germany, p. 933.

[11] Herguth, A. et al. 2006, "Avoiding boron-oxygen related degradation in highly boron doped Cz silicon",

"It seems as if the presence of the n^+ emitter during the fast-firing step negatively affects the bulk lifetime."

Proc. 21st EU PVSEC, Dresden, Germany, p. 530.
[12] Dullweber, T. et al. 2017, "Bifacial PERC+ solar cells and modules: An overview", *Proc. 33rd EU PVSEC,* Amsterdam, The Netherlands, pp. 649–656.
[13] Walter, D., Lim, B. & Schmidt, J. 2016 "Realistic efficiency potential of next-generation industrial Czochralski-grown silicon solar cells after deactivation of the boron–oxygen-related defect center", *Prog. Photovolt: Res. Appl.,* Vol. 24, No. 7, pp. 920–928.
[14] Palmer, D.W., Bothe, K. & Schmidt, J. 2007, "Kinetics of the electronically stimulated formation of a boron-oxygen complex in crystalline silicon", *Phys. Rev. B,* Vol. 76, p. 035210.
[15] Richter, A. et al. 2012, "Improved quantitative description of Auger recombination in crystalline silicon", *Phys. Rev. B,* Vol. 86, p. 165202.
[16] Lim, B. et al. 2018, "LID-Free PERC + solar cells with stable efficiencies up to 22.1%", *Proc. 35th EU PVSEC,* Brussels, Belgium, pp. 359–365.
[17] Walter, D.C. et al. 2014, "Lifetimes exceeding 1ms in 1-Ω cm boron-doped Cz-silicon", *Sol. Energy Mater. Sol. Cells,* Vol. 131, pp. 51–57.
[18] Dullweber, T. et al. 2016, "PERC+: Industrial PERC solar cells with rear Al grid enabling bifaciality and reduced Al paste consumption", *Prog. Photovolt: Res. Appl.,* Vol. 24, No. 12, pp. 1487–1498.
[19] Brendel, R. 2012, "Modeling solar cells with the dopant diffused layers treated as conductive boundaries", *Prog. Photovolt: Res. Appl.,* Vol. 20, No. 1, pp. 31–43.
[20] Fell, A. 2012, "A free and fast three-dimensional/two-dimensional solar cell simulator featuring conductive boundary and quasi-neutrality approximations", *IEEE Trans. Electron Dev.,* Vol. 60, No. 2, pp. 733–738.
[21] Brendel, R. et al. 2016, "Breakdown of the efficiency gap to 29% based on experimental input data and modeling", *Prog. Photovolt: Res. Appl.,* Vol. 24, No. 12, pp. 1475–1486.
[22] Kleekajai, S. et al. 2006, "Concentration and penetration depth of H introduced into crystalline Si by hydrogenation methods used to fabricate solar cells", *J. Appl. Phys.,* Vol. 100, No. 9, p. 093517.
[23] Hamer, P. et al. 2018, "Modelling of hydrogen transport in silicon solar cell structures under equilibrium conditions", *J. Appl. Phys.,* Vol. 123, No. 4, p. 043108.

About the Authors

Dr. Bianca Lim joined ISFH in 2007 to work on boron–oxygen-related recombination centres. After receiving her Ph.D. in 2011, she was a project leader at ISFH. In 2015 she joined the Solar Energy Research Institute of Singapore (SERIS) to develop ion-implanted p- and n-type Si solar cells. She returned to ISFH in 2017 and is currently working on p-PERC solar cells as well as on BIPV.

Agnes Merkle studied physics at the University of Bucharest, Romania, where she specialized in biophysics. She joined ISFH in 1996, carrying out R&D work on several high-efficiency solar cell concepts. Her current research focuses on the drop-in implementation of passivating contacts in the current PERC process flow.

Prof. Dr. Robby Peibst is head of the emerging solar cell technologies R&D group at ISFH, and holds a professorship at the MBE institute at Leibniz University Hanover. His current research work focuses on passivating contacts based on doped polycrystalline silicon layers deposited on thin passivating interface oxides (POLO, poly-Si on oxide), including process development, principle studies and implementation in Si single-junction and Si bottom cells for tandem structures.

Dr. Thorsten Dullweber is head of the industrial solar cells R&D group at ISFH. His research work focuses on high-efficiency industrial-type PERC and bifacial PERC+ silicon solar cells. Before joining ISFH in 2009, Thorsten worked as a project leader for DRAM memory chips at Infineon Technologies AG. He received his Ph.D. in 2002 for research on Cu(In,Ga)Se_2 thin-film solar cells. He is a member of the scientific committees of the EU PVSEC and SNEC conferences, and of the editorial advisory board of Photovoltaics International.

Yichun Wang received an M.S. in electrical engineering in 2010 from the University of Kentucky, USA, and a B.S. in electrical engineering in 2007 from Northwestern University, China. She joined LONGi Green Energy Technology Co., Ltd. in 2014, and is currently the director of application engineering and key customer service in the Silicon Wafer Business Unit, where her responsibilities include technical/product quality support and supervising technical collaboration projects with global institutes and R&D corporations.

Enquiries
Bianca Lim
Institute for Solar Energy Research Hamelin (ISFH)
Am Ohrberg 1, D-31860 Emmerthal
Germany

Tel: +49-5151-999-403
Email: b.lim@isfh.de